Delft University of Technology
Faculty of Electrical Engineering, Mathematics and Computer Science
Delft Institute of Applied Mathematics

Modelling of heat transfer by radiation

(Modelleren van warmtetransport door straling)

Thesis submitted to the
Delft Institute of Applied Mathematics
in partial fulfillment of the requirements

for the degree

BACHELOR OF SCIENCE
in
APPLIED MATHEMATICS

by

HANS DE MUNNIK

Delft, Nederland
August 2021

BSc report APPLIED MATHEMATICS

"Modelling of heat transfer by radiation"

("Modelleren van warmtetransport door straling")

HANS DE MUNNIK

Delft University of Technology

Supervisor

Dr. D.J.P. Lahaye

Committee

Dr. ir. J. Bierkens

August, 2021 Delft

Abstract

Heat transfer by radiation is something you experience everyday: when walking outside in the sun or when cooking your diner. This thesis provides understandable models of the role that radiation plays in the transfer of heat. By studying literature we developed a mathematical basis for the heat transfer model, where we discuss diffusive, convective and radiative heat transfer, the weighted sum of grey gases and the chosen solving method: the discrete ordinates method. Using CONVERGE CFD and MATLAB software, we present several one- and three-dimensional simulations of a furnace in which we consider different conditions. The overall conclusion is that radiation transports heat from places with high temperatures to their cooler surroundings, where also conditions as isolation, wall emissivity and gas mixture play an important role.

Samenvatting

Warmtetransport door straling is iets waar je elke dag mee te maken hebt: van een heerlijke wandeling in de zon tot het koken van je avondeten. Deze scriptie presenteert begrijpelijke modellen die de rol van straling in warmtetransport duidelijk maken. Door middel van literatuurstudie zetten we een wiskundige basis op voor het warmtetransport model, waar we diffusie, convectie en straling bespreken, alsmede het 'weighted sum of grey gases' model en de gekozen oplossingmethode: de 'discrete ordinates method'. Met behulp van de CONVERGE CFD en MATLAB software, hebben we diverse een- en drie-dimensionale simulaties van een oven gemaakt, waarin we verschillende omstandigheden nabootsen. De algemene conclusie is dat straling warmte transporteert van een warme omgeving naar een koelere omgeving, waar ook voorwaarden als isolatie, wandemissiviteit en de gassamenstelling een belangrijke rol spelen.

Contents

1
Introduction

Radiation. Most people start to get nervous by hearing this word. We all know the frightening stories about high radiation levels and their consequences. But maybe you are now thinking about something closer to you, like the way the sun is powering the climate system and heating up the earth through radiation. Also in your everyday life, you are probably facing radiation: when you are cooking, the stove is hot and thereby emits radiation in the form of electromagnetic waves, which changes the temperature of both the stove and its surroundings.

On a bigger scale, this radiative transport plays a very important role in the modelling of heat transfer in mixtures of gases at high temperatures. Despite its domi-

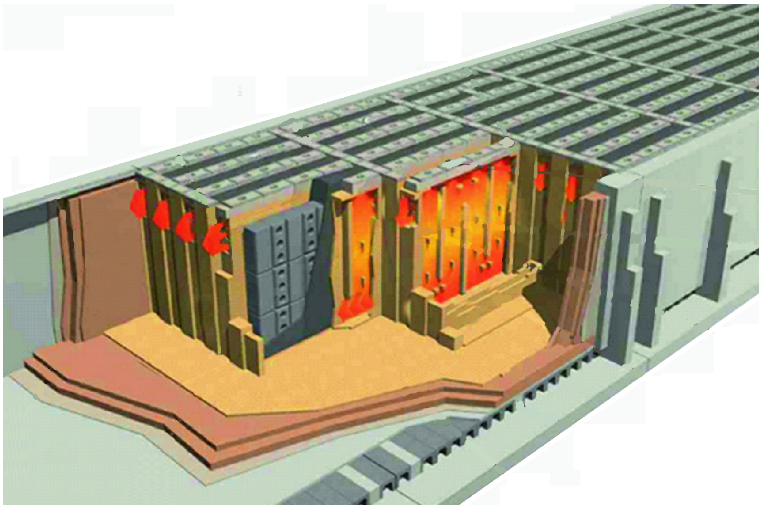

Figure 1.1: Overall geometry of an anode baking furnace (MMMS, 2020)

nant role in combustion systems, little attention is being paid at modelling radiation. However, ignoring radiation can lead to serious overprediction of temperatures. The design of fuel efficient internal combustion engines and the operation of large industrial furnaces critically rely on accurate radiative heat transfer models.

In this thesis, we will focus on modelling heat transfer by radiation in large industrial furnaces and making this understandable. The anode baking furnaces we target are used in for instance the production of cement and steel (figure 1.1). The understanding of how the heat produced by the combustion is transported throughout the furnace by radiation will in the future allows to steer the combustion process and to implement measures to reduce fuel consumption and pollutant emissions. On top of that, the understanding of heat transfer by radiation helps to quantify the heat transfer to the raw materials being processed in the furnace.

To make efficient calculations and keep the focus on the modelling of heat transfer by radiation, instead of peripheral matters, we made some assumptions in this research. At first, we won't make use of the flow of fluid in the furnace, unless mentioned differently. Besides, we consider the radiation to be non-scattering and in a grey atmosphere (the absorption coefficient κ is constant for all frequencies of radiation).

In chapter 2, the first part of this thesis, we provide some theory on heat transfer, which is needed for setting up the models in the next chapters. An important part of this chapter will be the discrete ordinates method. This method discretizes the spatial dependence of the radiative intensity by considering a set of angular directions. In each direction, a transport equation for the radiative intensity has to be solved to be able to obtain the radiative flux. We will also look into the weighted sum of grey gases model, to discuss the role of the gas mixture itself in the heat transfer.

In chapter 3, we will use CONVERGE CFD to look into radiation modelling in a large industrial furnace and make different simulations. CONVERGE CFD is a leading computational fluid dynamics software for simulating three-dimensional fluid models, used by the motor racing industry, automotive companies, governments and universities.

In chapter 4, we write one-dimensional implementations in MATLAB to explain the three-dimensional results from CONVERGE CFD. Therefore we duplicated the CONVERGE CFD models as much as possible in MATLAB, so that we can see what happens in the calculation process.

In chapter 5, the conclusion, we will sum up all discussed results from the previous chapters to give a short overview of what we accomplished in this research.

This thesis is written as part of the bachelor's degree in Applied Mathematics at the Delft University of Technology.

2

Theory on heat transfer

This chapter will provide some necessary theory on fluid dynamics, which we will use to run simulations in the next chapters of this thesis. In chapter 2, we will develop a mathematical basis for the heat transfer model.

Heat transfer is the exchange of thermal energy (heat) from a high temperature location towards a location with lower temperature, according to the second law of thermodynamics (Versteeg, 2007, p. 301). In engineering science there are three fundamental modes of heat transfer (figure 2.1):

- Diffusion (conduction): the transfer of energy between two objects which are in physical contact.
- Radiation: the transfer of energy between two objects which are not in physical contact, due to the emission of electromagnetic radiation.
- Convection: the transfer of energy between a fluid and its environment, caused by fluid motion.

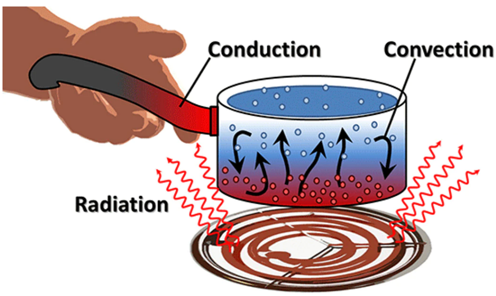

Figure 2.1: Modes of heat transfer (UWSP, 2021)

As we can see, there are three modes of heat transfer: convection, diffusion (section 2.1) and radiation (section 2.2). After discussing these heat transfer models, we will look into the method we will be using to solve the radiative heat transfer model: the discrete ordinates method (section 2.3). We conclude this chapter with an extension to the model (the weighted sum of grey gases), which makes it possible to take a changing mixture of gases into account (section 2.4).

2.1. Diffusive convective heat transfer

As mentioned before, diffusion (conduction) is the transfer of energy between two objects which are in physical contact. Neighboring atoms or molecules collide, after which the faster one loses some of its kinetic energy to the slower one. On the other hand, convection is caused by the flow of a fluid. The convection-diffusion equation describes temperature fluctuations in materials undergoing convection or diffusion. This process depends on the temperature gradient and the properties of the materials involved. The partial differential equation can be written as

$$c_p \rho \frac{\partial T}{\partial t} = \nabla(k \nabla T) - v \nabla T + S, \tag{2.1}$$

where $T(\mathbf{r}, t)$ is the temperature (in K) of the material at location $\mathbf{r} = (x, y, z)$. Furthermore, c_p denotes the specific heat capacity (in J kg^{-1} K^{-1}), ρ is the density of the diffusing material (in kg m^{-3}) and k denotes its thermal conductivity (in W m^{-1} K^{-1}). v (in m s^{-1}) is the velocity of the fluid, which depends on time and space. In this thesis, we let $v = 0$. S is a source-sink term (in W m^{-3}), where heat can be generated or be lost.

2.2. Radiative heat transfer

2.2.1. Definitions

Thermal radiation is caused by an object emitting energy in the form of electromagnetic waves. All materials emit and absorb electromagnetic waves continuously, but the strength depends on its temperature. Thermal radiation does not need a medium for its transfer, which makes it of great importance in vacuum and space applications as well.

Nevertheless, radiation modelling is a tough task, since its principal variable, the photon intensity $I(\mathbf{r}, \mathbf{s})$ is a function of space ($\mathbf{r}$) and direction ($\mathbf{s}$). Very often, combustion models make only use of convection, but since the temperatures generated by the chemical reactions are so high, radiative heat fluxes are of similar order of magnitude, which is why radiation is crucial to take into account when modelling combustion. Before we can state the radiative transport equation, we need to give some definitions and formulas.

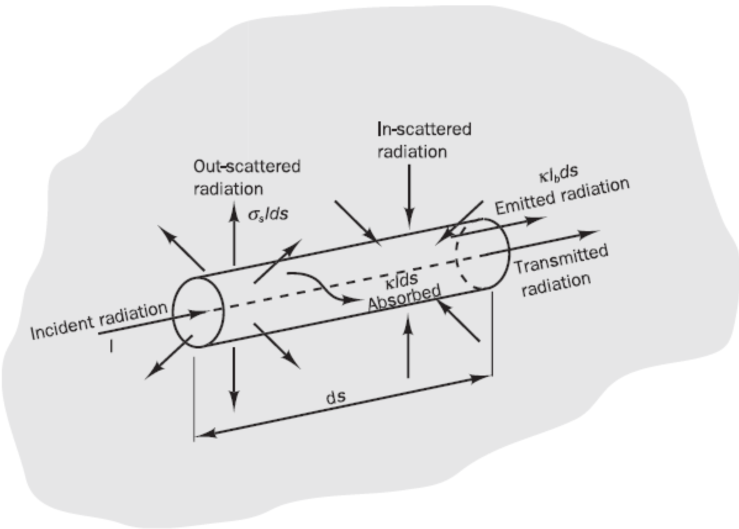

Figure 2.2: Schematic of interactions (Versteeg, 2007, p. 419)

A black body is a (theoretically idealized) physical body which absorbs all electromagnetic radiation. For such a black body its emissive power E_b (in W m^{-2}) is related to its temperature to its temperature by

$$E_b = \sigma T^4, \tag{2.2}$$

where σ denotes Stefan-Boltzmann's constant ($5.67051 \cdot 10^{-8}$W m^{-2} K^{-4}). We can also express this black body emissive power as a non-directional black body intensity:

$$I_b = \frac{E_b}{\pi}. \tag{2.3}$$

There may be interactions between radiation and the participating fluid medium (absorption, transmission, emission or scattering). Figure 2.2 shows these interactions by making use of the medium's absorption coefficient κ (in m^{-1}) and its scattering coefficient σ_s (in m^{-1}). The extinction coefficient β is the sum of these two coefficients. The emitted intensity I_f of such a participating fluid medium is given by

$$I_f = \kappa I_b. \tag{2.4}$$

Due to the radiative properties of the participating fluid medium, additional heat fluxes may appear as an extra source or sink in the energy equation. To compute this radiative heat flux, we first need to determine the intensity $I(\mathbf{r}, \mathbf{s})$ (in W m^{-2} sr^{-1}), which varies with direction ($\mathbf{s}$).

2.2.2. The equation of transfer

For obtaining the radiative transfer equation (RTE), we make an energy balance on the radiative energy in the direction $\mathbf{s}$ during a small increment of time. The energy balance is found by summing up the emitted energy $(+)$, the absorbed energy $(-)$, the out-scattered energy $(-)$ and the in-scattered energy $(+)$:

$$I(\mathbf{r}+d\mathbf{r},\mathbf{s},t+dt)-I(\mathbf{r},\mathbf{s},t)=\kappa I_b(\mathbf{r},t)d\mathbf{r}-\kappa I(\mathbf{r},\mathbf{s},t)d\mathbf{r}-\sigma_s I(\mathbf{r},\mathbf{s},t)d\mathbf{r} + \frac{\sigma_s}{4\pi}\int_{4\pi} I_-(\mathbf{s}_i)\Phi(\mathbf{s}_i,\mathbf{s})\ d\Omega_i d\mathbf{r}. \tag{2.5}$$

$I_-(\mathbf{s})$ denotes the incident intensity at a position $\mathbf{s}$ and $I_+(\mathbf{s})$ gives its outgoing intensity. $\Phi(\mathbf{s}_i,\mathbf{s})$ is called the scattering phase function and describes the distribution of the scattered intensity. As stated in chapter 1, we consider the scattering coefficient $\sigma_s = 0$, which eliminates the integral.

Since radiation can be seen as electromagnetic waves, its velocity of propagation is the speed of light c $(3.0\cdot 10^8$ m s$^{-1})$. In equation 2.5 we are following a path from $\mathbf{r}$ to $\mathbf{r}+d\mathbf{r}$ with velocity c, which is why $d\mathbf{r}$ and $d\mathbf{t}$ are related through $d\mathbf{r} = c\ d\mathbf{t}$ (Modest, 2003, p. 269).

After some calculations and simplifications, we can write the radiative transfer equations as follows:

$$\frac{1}{c}\frac{\partial I(\mathbf{r},\mathbf{s},t)}{\partial t}+\frac{\partial I(\mathbf{r},\mathbf{s},t)}{\partial s}=\kappa I_b(\mathbf{r},t)-\kappa I(\mathbf{r},\mathbf{s},t). \tag{2.6}$$

As mentioned before, radiaton travels with the speed of light, which is at least 10^5 times faster than the speed of sound in fluid mediums. Hence, heat exchanges by radiation are always in quasi-steady state. By assumption the intensities do not depend on frequency and considering the quasi-steady state, we can also eliminate the time-dependence. Hence, equation 2.6 can be rewritten as

$$\frac{\partial I(\mathbf{r},\mathbf{s})}{\partial s}=\kappa I_b(\mathbf{r})-\kappa I(\mathbf{r},\mathbf{s}). \tag{2.7}$$

Equation 2.7 is a first order differential equation and therefore needs one boundary condition. The boundary condition applies to the boundary where the angle between the surface normal $\mathbf{n}$ and direction $\mathbf{s}$ is less than $\frac{\pi}{2}$. The most popular boundary condition in this kind of radiative transfer problems is the sum of the emitted heat flux and the reflected heat flux, where we assume that the surface is non-transmissive. Hence, the inflow at position $\mathbf{r}_w$ along direction $\mathbf{s}$ is

$$I(\mathbf{r}_w,\mathbf{s})=\epsilon I_b(\mathbf{r}_w)+\frac{1-\epsilon}{\pi}\int_{\mathbf{n}\cdot\mathbf{s}_i<0} I_-(\mathbf{r}_w,\mathbf{s}_i)\mathbf{n}\cdot\mathbf{s}_i\ d\Omega_i, \tag{2.8}$$

where $\mathbf{n}\cdot\mathbf{s}_i$ is the cosine of the angle between any incoming direction $\mathbf{s}_i$ and the surface normal. ϵ denotes the surface emissivity: the ratio of heat flux emitted by a surface compared to a black surface.

2.2.3. Radiative heat flux

Now that we can calculate all intensities, we want to transform the total incident intensity and total outgoing intensity to a radiative source term for the energy equation. The net radiative heat flux (q_r) is given by substracting the outgoing heat flux (q_+) from the incident heat flux (q_-). Once we know all directional intensities, we can calculate both heat fluxes by integrating its corresponding intensities (Versteeg, 2007, p. 422):

$$q_-(\mathbf{r}) = \int_{2\pi} I_-(\mathbf{r},\mathbf{s})\mathbf{s}\cdot\mathbf{n}\, d\Omega, \tag{2.9}$$

$$q_+(\mathbf{r}) = \int_{2\pi} I_+(\mathbf{r},\mathbf{s})\mathbf{s}\cdot\mathbf{n}\, d\Omega. \tag{2.10}$$

After evaluating q_r, the radiative source term for the energy equation can be calculated from:

$$S_{h,rad} = \nabla\cdot\mathbf{q}_r(\mathbf{r}). \tag{2.11}$$

We can now insert $S_{h,rad}$ into equation 2.1 as a source-sink term.

2.3. Discrete ordinates method

Except for a couple of idealised cases, an exact analytical solution is not available for the radiative transfer equation. We do notice that we need an iterative method to solve the RTE, since the incident intensities in equation 2.7 and 2.8 are unknown at the start of the calculation. Initially we use assumed values of the surface intensities and after each iteration we can evaluate the incident intensities again. Also we are looking for a method which is accurate with anisotropic radiative, since the radiative transfer equation has to be evaluated in every direction.

Over time a lot of methods have been developed to solve the radiative heat equation numerically. Literature study on reviews in Selçuk (1996), Modest (2003) and Versteeg (2007) revealed several benefits and pullbacks of a number of general-purpose radiation models. We list the most popular algorithms below to be able to make a considered choice for a method:

- P_N (P_1) method: according to Modest, the convergence of this method may fail in case of optical thickness and is also not accurate in case of anisotropic radiative intensity.
- Monte Carlo method: this algorithm is too expensive in terms of computational time - it requires very much storage capacity and very large amounts of computing resources and is therefore not suitable for general-purpose computational fluid dynamics calculations. Meanwhile, the discrete transfer method is even around 500 times faster than the Monte Carlo method.

- Discrete transfer method: this method is limited to isotropic scattering as stated by Versteeg. Moreover, Modest claims that the discrete transfer method uses more cumbersome beam tracing, which causes inaccuracies and according to Selçuk, this method is even shows one of the greatest average deviations.
- Discrete ordinates method: this algorithm is suitable for anisotropic radiative intensities and applicable to scattering and non-scattering problems. Selçuk even claims this method performs as one of the most accurate, combined with a high degree of computational economy in terms of CPU time.

2.3.1. Discrete ordinates equations

In consequence, we choose the discrete ordinates method (DOM), based on discretizing both the space domain and the angular variables specifying the direction of radiation, as a solving method. Instead of solving for all possible directions, the DOM solves the equation of transfer for a set of n different directions (figure 2.3). The integrals over directions are now replaced by numerical quadrature.

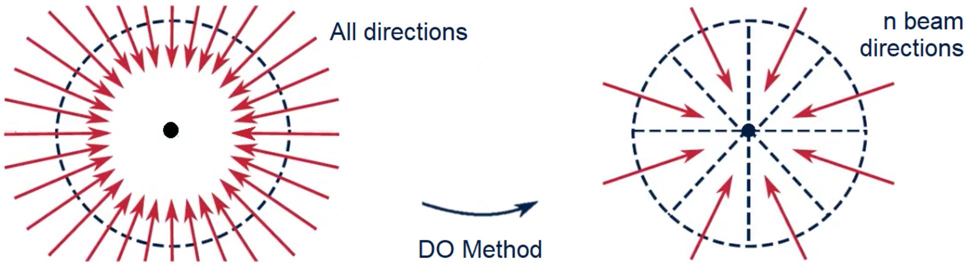

Figure 2.3: The discrete ordinates method (Fluid Mechanics 101, 2020)

When using the discrete ordinates method to solve the radiative transfer model (section 2.2), the equation of transfer (equation 2.7) will be approximated by

$$\frac{\partial I(\mathbf{r},\mathbf{s}_i)}{\partial s} = \kappa I_b(\mathbf{r}) - \kappa I(\mathbf{r},\mathbf{s}_i), \tag{2.12}$$

for $i = 1, 2, ..., n$. Since the governing equation is first order, every beam traveling in a direction $\mathbf{s}_i$ needs exactly one boundary condition. This boundary condition (equation 2.8) becomes:

$$I(\mathbf{r}_w,\mathbf{s}_i) = \epsilon I_b(\mathbf{r}_w) + \frac{1-\epsilon}{\pi} \sum_{\mathbf{n}\cdot\mathbf{s}_j<0} w_j I_-(\mathbf{r}_w,\mathbf{s}_j)|\mathbf{n}\cdot\mathbf{s}_j|, \tag{2.13}$$

where w_j are quadrature weights associated with the directions $\mathbf{s}_j$. In other words, equation 2.12 will be solved for a set of n different directions $\mathbf{s}_i$ and therefore approximated by a set of n equations, subject to corresponding boundary conditions.

Once the intensities have been calculated, we can determine the net radiative heat fluxes by its definition (equation 2.9 and 2.10):

$$\mathbf{q}_r(\mathbf{r}) \quad = \quad \sum_{j=1}^{n} w_j I_j(\mathbf{r}, \mathbf{s})\ \mathbf{s} \cdot \mathbf{n}. \tag{2.14}$$

The radiative source term can now be calculated from equation 2.11:

$$S_{h,rad} = \nabla \cdot \mathbf{q}_r(\mathbf{r}) = 4\pi\kappa I_b - \kappa \sum_{j=1}^{n} w_j I_j(\mathbf{r}, \mathbf{s}). \tag{2.15}$$

2.3.2. Discrete ordinate directions

When using the discrete ordinates method, the choice of quadrature scheme is arbitrary. Its accuracy depends a lot on the geometry of the model. However, there are restrictions on the set of directions and also the preference to preserve symmetry plays a role. Another term for the DOM is the S_N method, were the number of directions n is correlated with N by $n = N(N+2)$ (so the S_2 set would consist of 8 directions).

The basis of obtaining the associated quadrature weights w_j is discussed in Modest (2003), who suggests various sets which satisfy the three moments equations which are stated in his book. These sets meet for instance the restriction to make the total sum of the quadrature weights w_j equal to the 4π solid angle and the preference to preserve symmetry (i.e., the set is invariant after any rotation of $90°$).

The set of discrete directions are spanning the total solid angle range of 4π and are given by $\mathbf{s}_i = \xi\mathbf{i} + \eta\mathbf{j} + \mu\mathbf{k}$, where $\mathbf{i}$, $\mathbf{j}$ and $\mathbf{k}$ are representing the unit vectors and ξ, η and μ are direction cosines (the cosine between the direction and its corresponding unit vector).

The set of coupled differential equations can be solved by discretization using the finite volume method (FVM) or the finite difference method (FDM). The FVM and the FDM are both methods to evaluate partial differential equations. For evaluating models with uniform mesh, they are identical in most cases. Since discretization is not the interest of this research, we will not elaborate on this topic.

2.4. Weighted sum of grey gases

As stated in the introduction, we work in a grey atmosphere, which indicates that the absorption coefficient κ is constant for all frequencies of incident radiation. When there is no change in mixture of gases in the timeframe of a model, we can work with a grey gas model, which assumes that the gas is grey and it uses an average absorption coefficient κ of all gases over the whole spectrum.

The concept of a weighted sum of grey gases (WSGG) replaces the nongrey gas in the radiative transfer equation by a number of grey gases, for which the intensities are calculated independently. The total flux can then be found by adding the intensities of all grey gases after multiplication with certain weight factors.

In general, different gases have different absorption coefficient, which results in a different composition of grey gases over time. Especially in combustion models, this approach is extremely useful, since the configuration of gases is continuously changing due to the combustion of methane:

$$\mathrm{CH_4} + 2\,\mathrm{O_2} \longrightarrow 2\,\mathrm{H_2O} + \mathrm{CO_2}. \tag{2.16}$$

For this reason, the concentrations of H_2O and CO_2 get higher during the combustion process, which will influence the rate of absorption in the composition of grey gases.

3

CONVERGE CFD simulations

Now that we have defined models for diffusive heat transfer and radiative heat transfer, we would like to run simulations to visualize the influence of radiation on the transfer of heat in a furnace. Using the CONVERGE CFD software is one way to do this. CONVERGE CFD is a leading computational fluid dynamics software for simulating three-dimensional fluid models.

The software package of Convergent Science, who claims that CONVERGE CFD is their absolute flagship product, consists of three steps. To start with, Converge Studio allows you to create a geometry, define boundaries and specify which physical models you want to use for your simulation. The next step is the solver, which runs your model on the grid and for the time steps you defined. At last, we can visualize the results by importing the solved simulation files in Tecplot 360 suite.

3.1. Geometry of the study model

After a lot of training, we were able to import and adapt an existing geometry of a study model for an anode baking furnace with burner (figure 1.1). In figure 3.1 you can see the burner at the center on top, the lateral air injection at the top right and the outlet at the bottom left - figure 3.2 shows the same geometry in three dimensional view. Figure 3.3 is showing the geometry from above, where we can see the burner (fuel inlet pipe) and the thickness of the geometry. All three figure are simplifications from the anode baking furnace (Nakate, 2021).

3

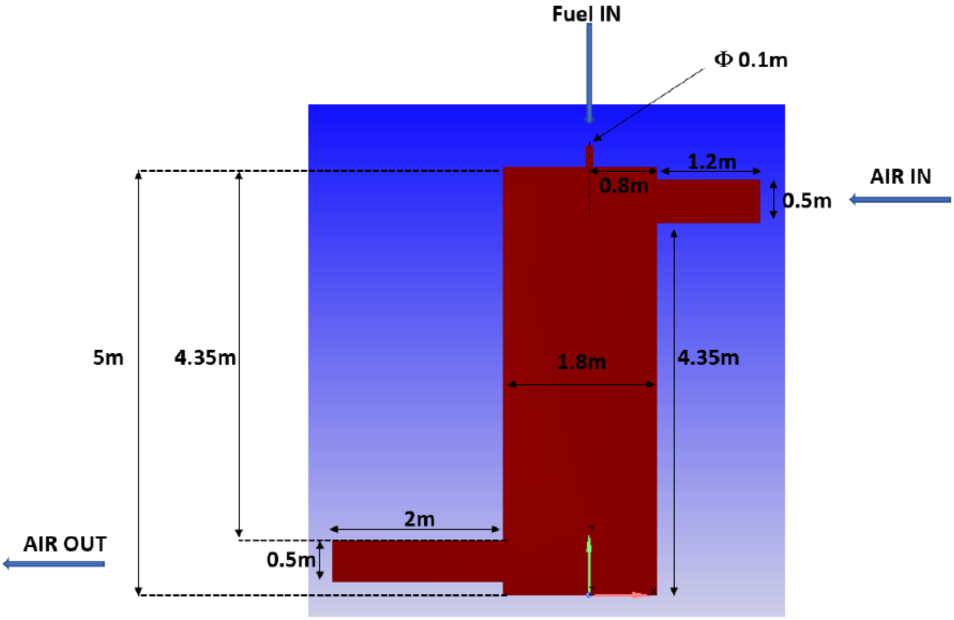

Figure 3.1: Schematic representation of the geometry of the study model

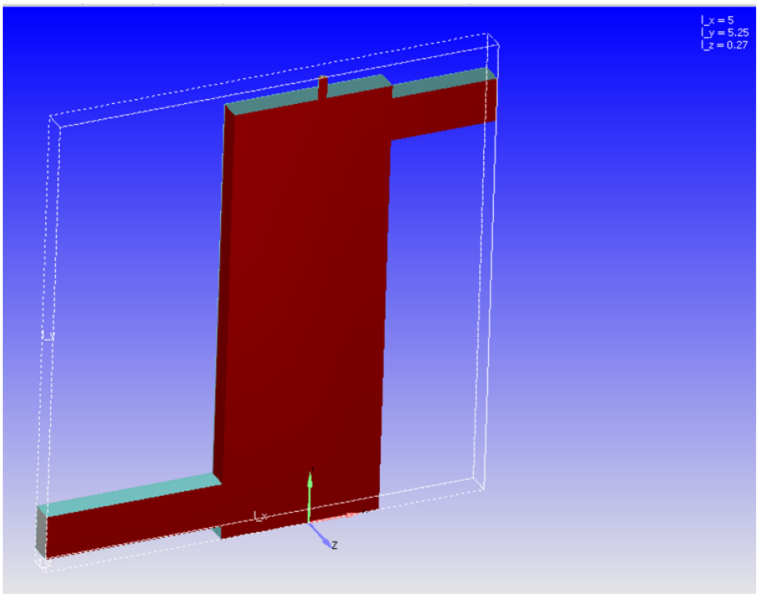

Figure 3.2: Three dimensional view on the study model's geometry

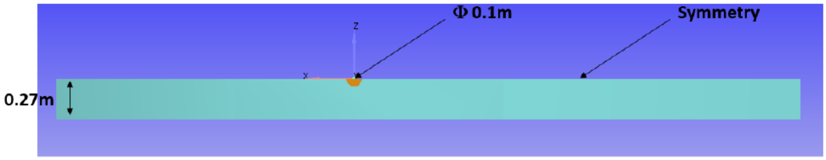

Figure 3.3: Top view of the above geometry

3.2. Simulations

The simulations we ran in CONVERGE CFD are all based on the geometry of the study model. We assigned Neumann boundary conditions for temperature on the walls and the outlet, which mean we don't allow heat flow through the walls of the furnace. Regarding the air inlet and fuel inlet, there is usually a flow of air and fuel into the furnace. In the first simulations we don't make use of fluid flow yet, so we set the velocity boundary conditions to zero and the temperature boundary conditions equal to 300 K (Dirichlet boundary condition). The furnace itself is filled with a simplified mixture of gases which approaches the compound of air: 78% N_2 and 22% O_2. The initial temperature in the whole furnace is 300 K.

In this subsection we describe the different simulations: diffusive heat transfer (subsection 3.2.1), radiative heat transfer (subsection 3.2.2), reflecting walls (subsection 3.2.3) and the weighted sum of grey gases (subsection 3.2.4). In this report we will present the simulations by showing slices of the XY-plane in the middle of the furnace, such that the source inside the furnace is visible. All observations will be discussed in chapter 4 by making use of a one-dimensional study.

3.2.1. Diffusive heat transfer

In this specific simulation, we are simplifying the combustion of methane by creating a box-shaped energy source in the furnace with the same amount of energy as the combustion heat of methane. The energy source only emits energy in the first 10 seconds of the simulation. After this time, we can see the process of heat transfer without a source. Heat transfer in this model only happens because of diffusion.

The results of this simulation (showing the temperature distribution after 1, 2, 4, 6, 10 and 20 seconds) can be found in figure 3.4. We can clearly see the box-shaped energy source just above the middle of the furnace heating up the volume. When the source stopped emitting energy (after 10 seconds), the temperature distribution in the furnace is now only changing very slowly. In the last plot (20 seconds) we can see there is still a temperature difference between the upper area and lower area of the furnace.

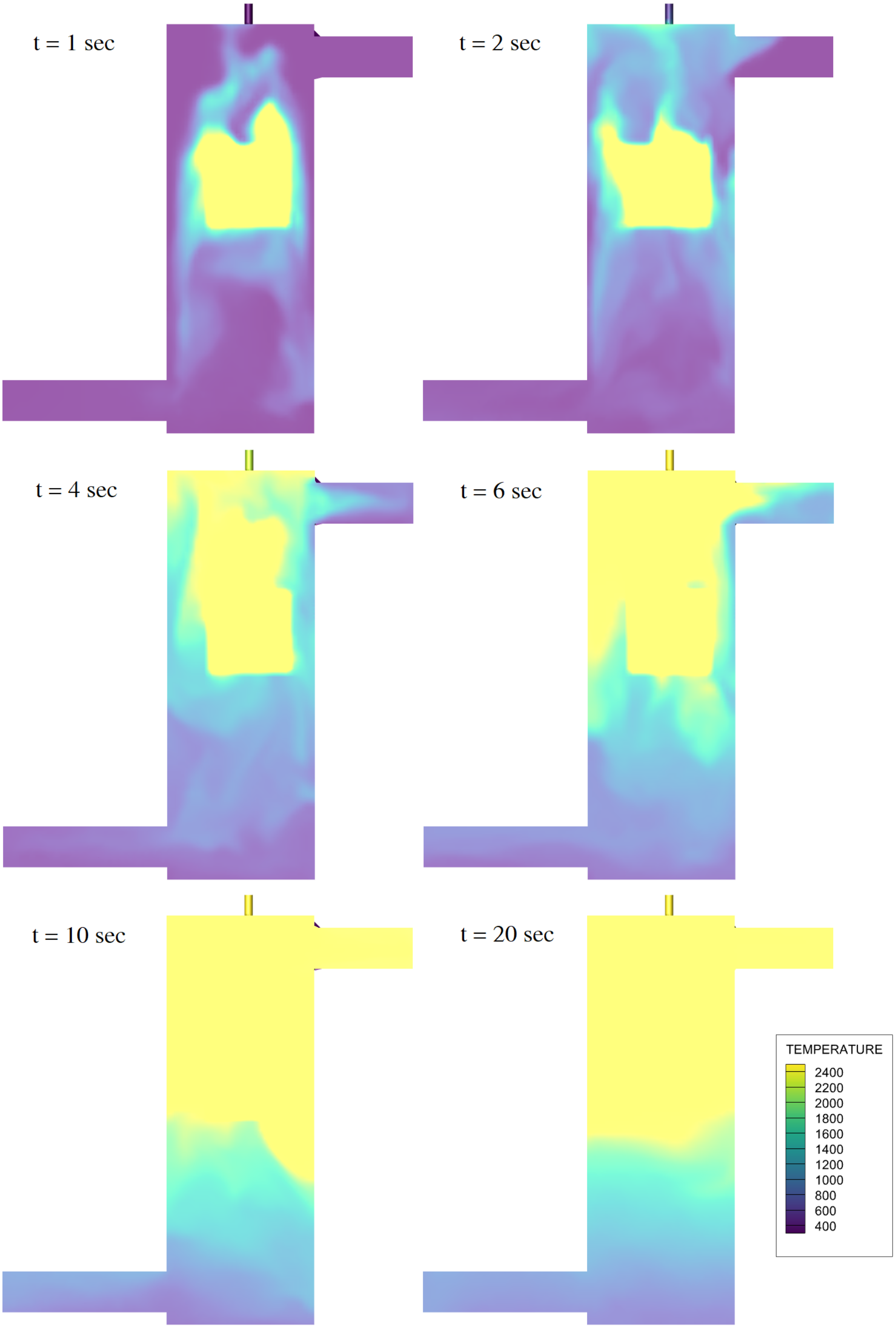

Figure 3.4: Simulation diffusive heat transfer

3.2.2. Radiative heat transfer

This simulation is an extension to subsection 3.2.1. In addition to previous subsection, with diffusion only, heat can now also be transferred by means of radiation. The radiative transfer equations are being solved using the discrete ordinates method in 8 directions.

Since the mixture of gases doesn't change during our simulation, it suffices to assign a constant value of the absorption coefficient κ to the grey gas in the furnace. We took the Planck mean absorption coefficient for air at 2000 K (Zhang (2001), Chmielewski (2015)) as a reference for the grey gas absorption coefficient: $\kappa = 0.5$.

All boundaries in the furnace have an emissivity equal to 1, which physically means that the surface is a perfect emitter of energy (black surface). The assigned value comes close to the emissivity of materials as rough concrete and galvanised steel.

The results of this simulation (showing the temperature distribution after 1, 2, 4, 6, 10 and 20 seconds) can be found in figure 3.5. In this figure we immediately notice the difference with the diffusive heat transfer simulation (figure 3.4). In the first two seconds we notice that the area around the energy source is different in two ways. At first, the direct surroundings of the source have a lower temperature in the radiative heat transfer simulation. Next, in figure 3.5, a bigger part of the furnace is already heated, which implies that heat is transferred faster in our second simulation.

Finally, in the 20-seconds-plot, we can see that there is almost a uniform temperature distribution along the furnace area. The cooling down of the center of the furnace is due to the transfer of heat to the colder area's (including areas in the 3D model we don't see in this figure), the absence of the energy source after $t = 10$ and the influence of the cooled boundaries at the two inlets.

3.2.3. Reflecting wall

The next simulation is similar to the one in subsection 3.2.2. The only difference is that we now assign a wall emissivity of 0 to the boundaries, which approaches the emissivity of materials as polished noble metal.

The results of this simulation (showing the temperature distribution after 1, 2, 4, 6, 10 and 20 seconds) can be found in figure 3.6. We can see an even faster heat transport than in figure 3.5, causing a more equally distributed temperature after 10 seconds. Because of the faster heat transport, we also observe a faster cooling down of the furnace in case of cooled walls (fuel inlet and air inlet).

3

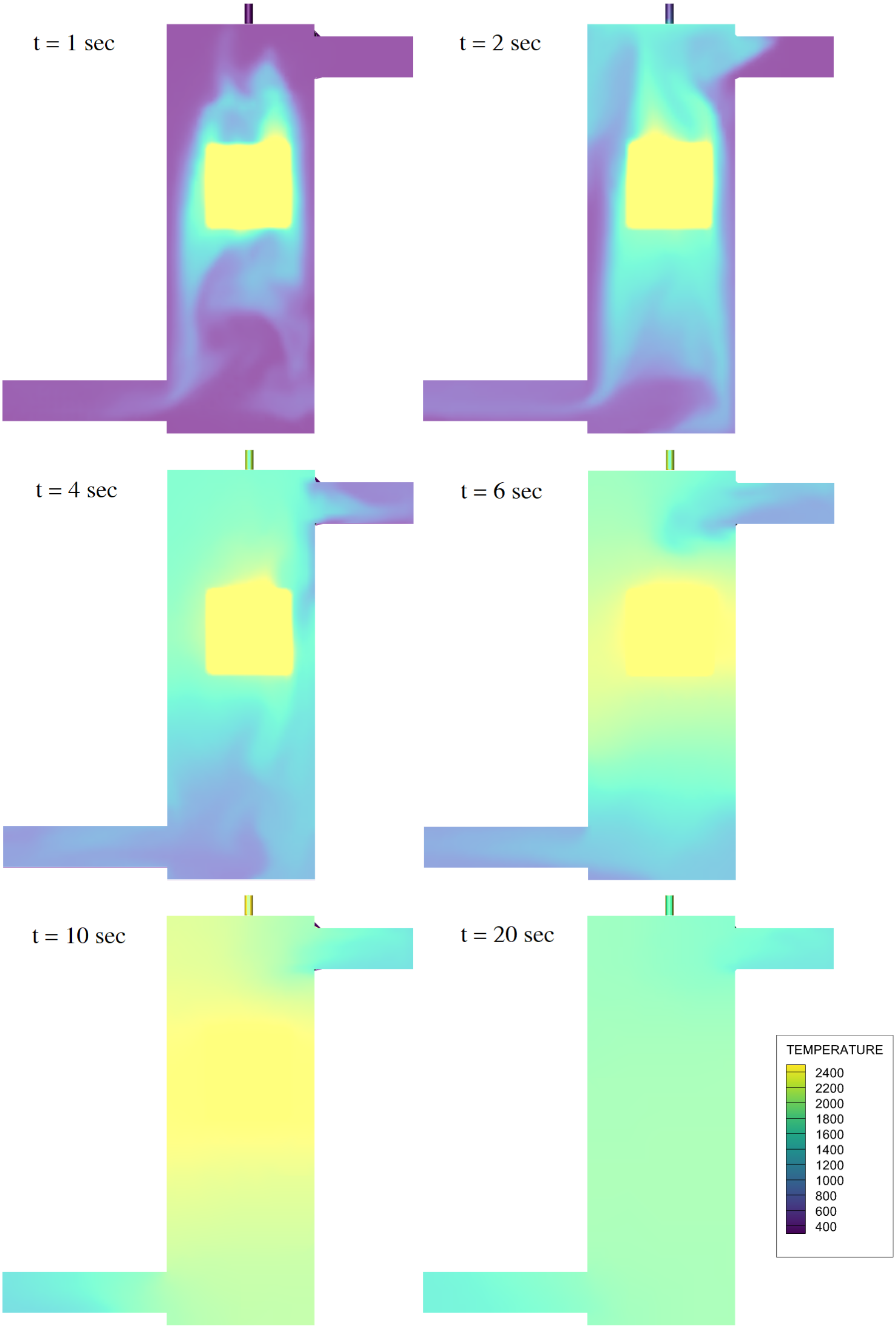

Figure 3.5: Simulation radiative heat transfer

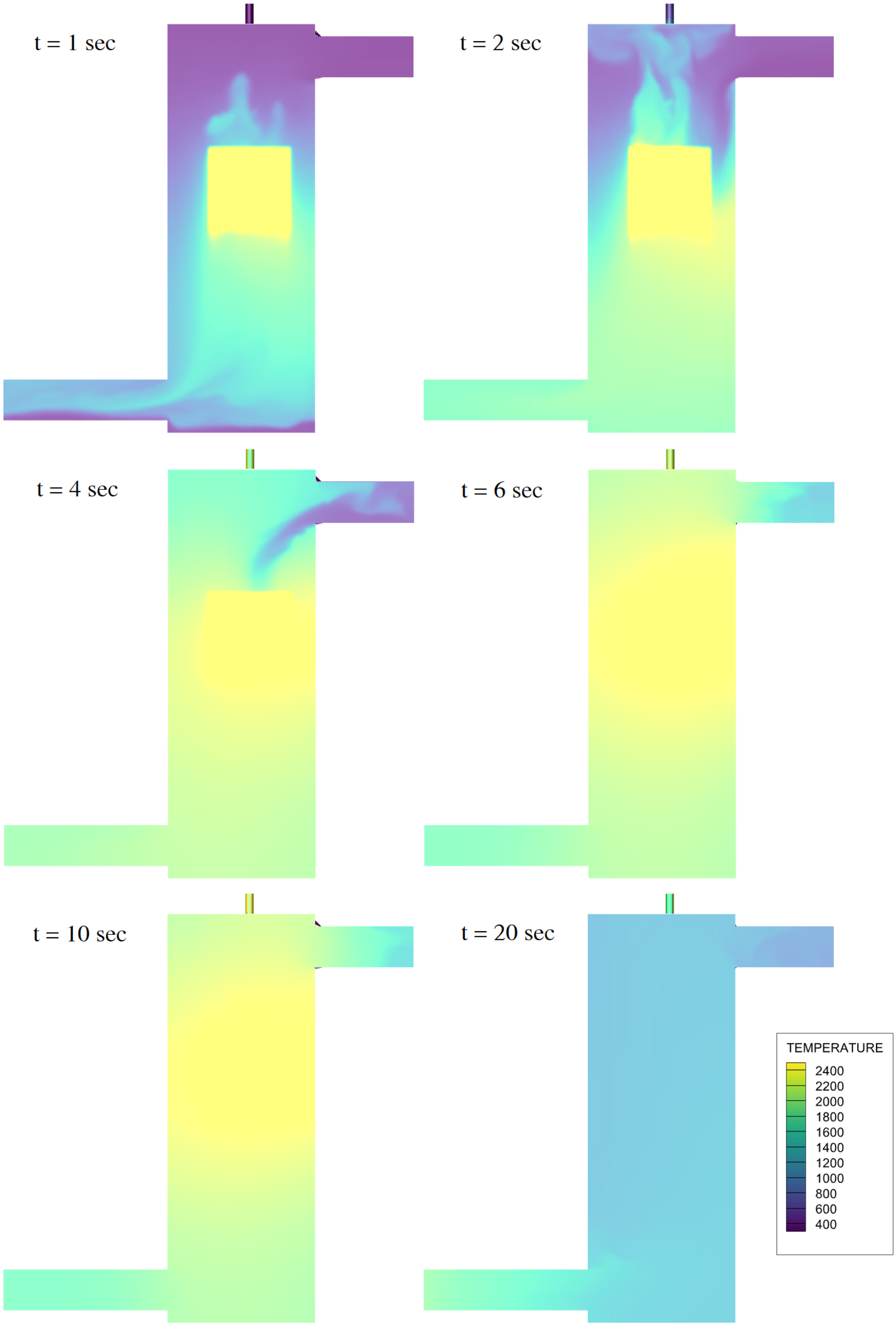

Figure 3.6: Simulation radiative heat transfer with reflecting walls

3.2.4. Weighted sum of grey gases

The FGM (Flamelet-Generated Manifold) is an accurate and efficient combustion chemistry reduction method, developed by the Combustion Technology Group of Eindhoven University of Technology. In this subsection we use the FGM case setup to simulate the furnace during the combustion of methane, where we use now the real chemical reaction (equation 2.16) instead of the box-shaped energy source. This subsection is the only simulation in this thesis where convection is being used.

The initial furnace temperature is 1.323 K, to make sure that it is warm enough for the combustion reaction to happen. The initial gas mixture did not change in comparison with the previous subchapters. The fuel inlet is now pumping methane ($\mathrm{CH_4}$) into the oven with a speed of 5 m s^{-1}. The air inlet makes sure there stays enough oxygen in the furnace to react with the methane by letting in hot air with a speed of 1.45 m s^{-1}. The outlet is transporting gas out of the furnace at a constant speed. In the first two seconds of the simulation, fuel (methane) will be flowing into the furnace. The combustion process starts after two seconds, when there is already a significant amount of methane gas present in the furnace.

The results of this simulation (showing the temperature distribution after 1, 2, 3, 4, 6 and 10 seconds) can be found in figure 3.7. We observe that the high mass fraction of methane in the furnace leads to a very high temperature in the beginning, after the combustion reaction has happened. Later on we see the balance between methane and oxygen restore, which is shown in the final plot (10 seconds). The highest mass fractions of O_2 can be found at the rightside of the furnace, which is why we see the combustion happening in this place.

Now we want to see what happens to the temperature distribution in the furnace when also radiation is taken into account concerning the transfer of heat. As stated in section 2.4, the weighted sum of grey gases model allows us calculate with a changing mixture of gases. During the combustion of methane, the concentrations of H_2O and CO_2 will get higher and influence the rate of absorption. Hence, we included the WSGG model into this simulation, where the absorption coefficients are based on the mass fractions of gases in the furnace.

The results of this simulation (showing the temperature distribution after 1, 2, 3, 4, 6 and 10 seconds) can be found in figure 3.8. We observe similar results as we did with the box-shaped energy: radiation leads to a lower maximum temperature and a faster transport of heat to cooler surroundings.

Since the WSGG model is applied, the absorption coefficient κ depends on the mass fractions of the gases. Literature demonstrates that, during the combustion process, κ is dominated by CO_2 and H_2O, which have significantly higher absorption coefficients the other gases (Chmielewski, 2015). The effect of this can be seen in figure 3.8: the outlet gas stream with high concentrations of H_2O and CO2 causes a faster transport of heat towards the outlet.

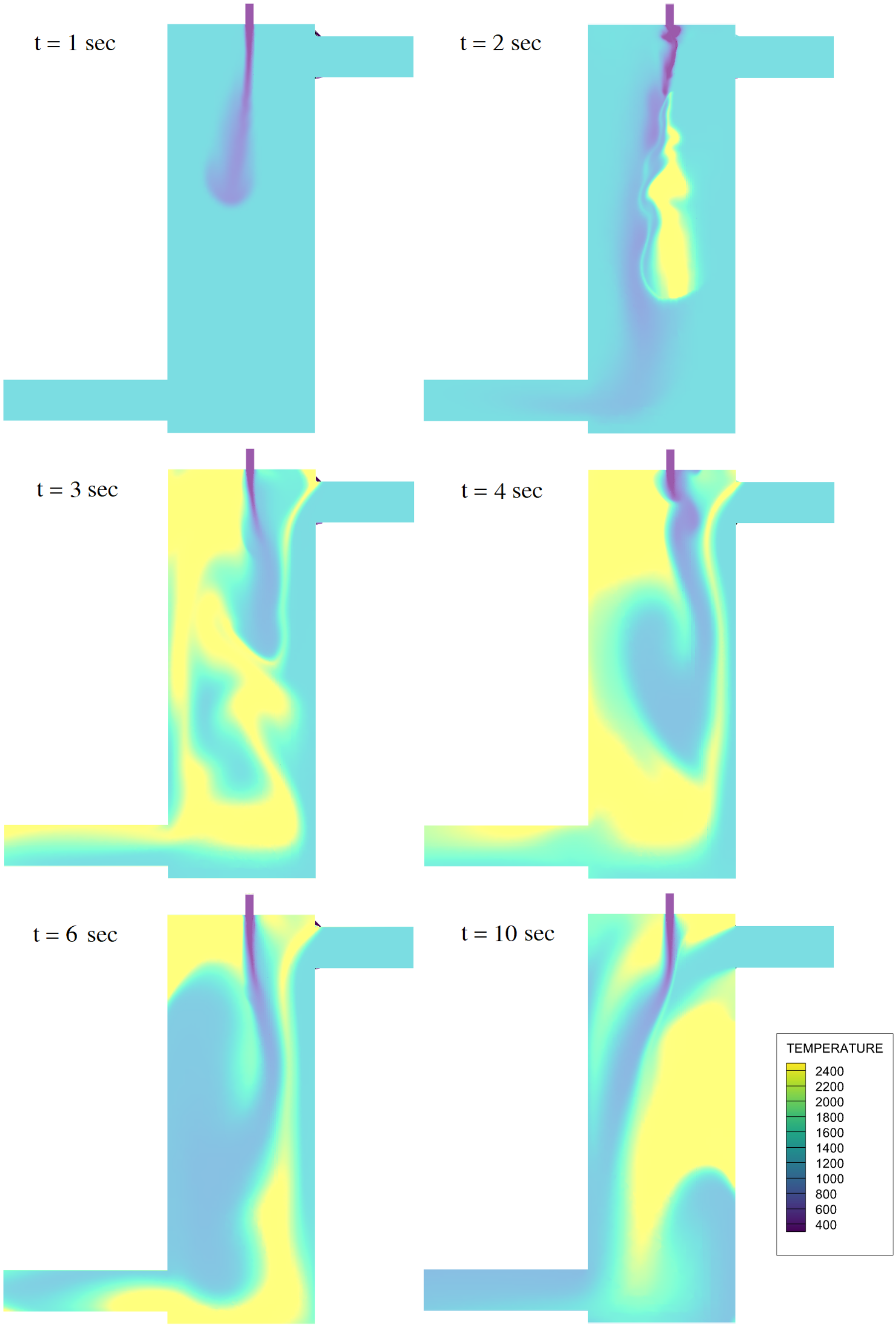

Figure 3.7: Simulation combustion of methane with convective-diffusive heat transfer

3

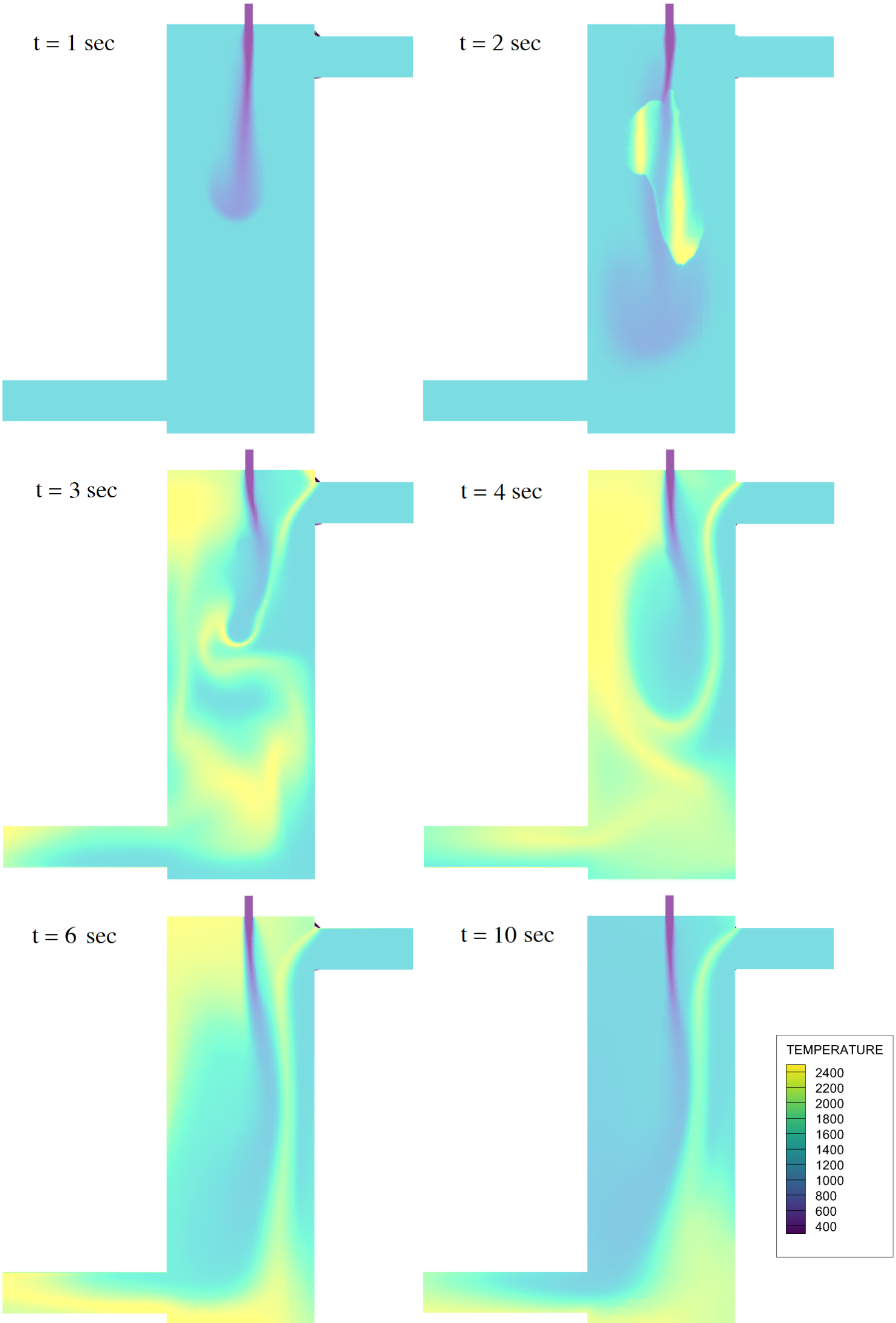

Figure 3.8: Simulation combustion of methane with radiative heat transfer

4

One-dimensional study

The computational time of the CONVERGE CFD software, which was used in chapter 3, could take up to multiple days for just one simulation. As a result of this, adapting the geometry of the furnace, varying conditions and changing physical models step-by-step took very long. Because of this computational time and to declare the results we have seen in the previous chapter, we made our own MATLAB implementation of the furnace in a one-dimensional space. This implementation is based on the used settings and methods from CONVERGE CFD.

Using this MATLAB implementation, we will explain the used models and discuss the results of the radiative heat model.

4.1. Diffusive heat transfer

As mentioned in chapter 2, heat exchanges by radiation always take plays in quasi-steady state. For this reason, we also consider the diffusive heat transfer in a steady state, which means that the temperature does not change any further due to diffusion. The furnace we will simulate in MATLAB is 1 meter in length and its initial temperature is, just like in section 3.1, 300 K.

To simulate a heat source in the middle of the furnace, caused by the combustion of methane, we used a heaviside step function with as value the combustion heat of methane $E = 35,8 \cdot 10^6$ J m^{-3}. Furthermore, we use air as the participating fluid. The model uses Dirichlet boundary conditions, which guarantees that the walls of the furnace stay at a temperature of 300 K.

The steady state solution (SSS) is given by

$$T(x) = -\frac{E}{2c_p\rho}\left[(x-0.4)^2H(x-0.4)-(x-0.6)^2H(x-0.6)\right] + \frac{E}{10c_p\rho}x + 300 \tag{4.1}$$

and is shown by the blue line in figure 4.1.

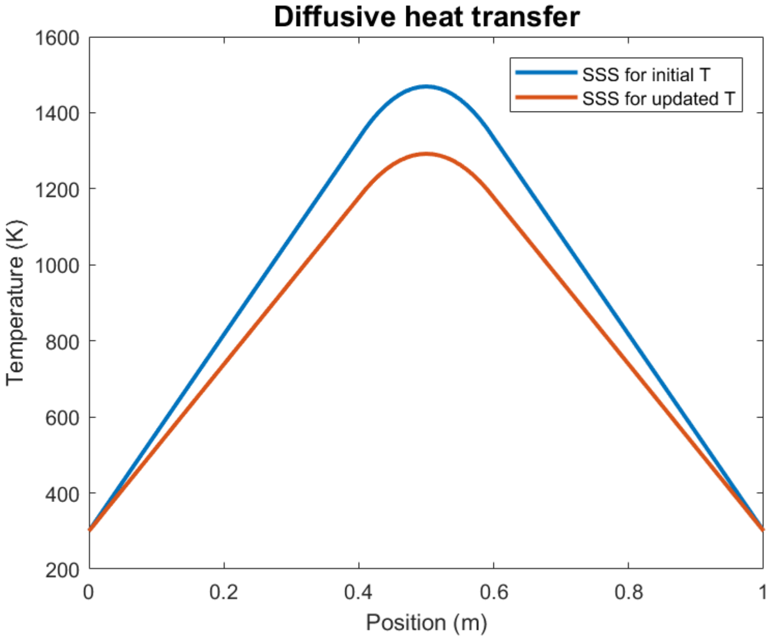

Figure 4.1: Diffusive heat transfer model

Considering that the physical properties of gases strongly depend on the temperature in the furnace, we made the diffusion calculation temperature dependent by exporting the CONVERGE CFD data files, import these data in MATLAB and evaluate the temperature at every grid point every iteration, after which the value of each physical property is determined. We see in the figure above the effect of an increasing conductivity due to the increasing temperature, which causes a faster heat transport and therefore a more flattened curve.

4.2. Radiative heat transfer

Starting with the steady state solution of the diffusive heat transfer model, we will perform an iteration to solve the radiative transfer equations. In each iterative step we evaluate the black body intensity in the furnace, after which we solve the radiative transport equations for both possible directions in a one-dimensional space. We use the same grey gas absorption coefficient and wall emissivity as in subsection 3.2.2 and give both directions, fulfilling the moments equations, quadrature weights $w_1 = w_2 = 2\pi$.

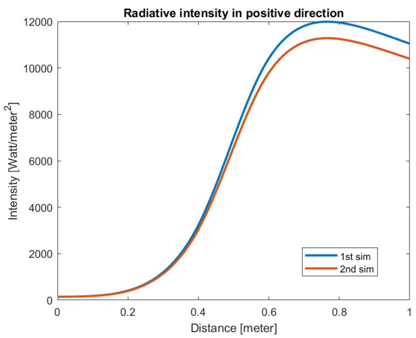

Figure 4.2: Radiative intensity in positive direction

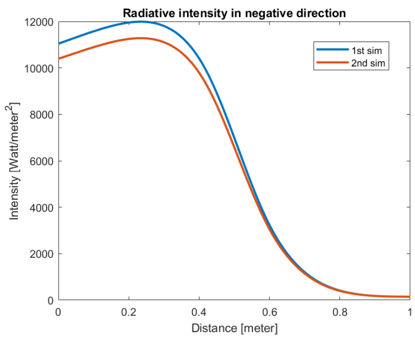

Figure 4.3: Radiative intensity in negative direction

The solutions of the radiative transport equations in figure 4.2 and 4.3 are showing the intensities in both directions. We can clearly see the top of the intensities moving away from the center, where the heat source is located, to the boundary its direction is pointing.

Subsequently, we use the calculated intensities and their corresponding quadrature weights to determine the radiative flux. This radiative flux will be used in the next iterative step to update the heat source term. We keep doing this until the solution has converged, where the heat source (the sum of the flame and the incident radiative heat flux) equals the total outgoing radiative heat flux.

We see in figure 4.4 that radiation slightly cools down the top of the temperature graph. This happens because radiative heat transfer is a strong function of the temperature (to the fourth power) and therefore the body with the highest temperature emits the most electromagnetic radiation. By emitting radiation, the body loses energy and cools down.

This energy is transported to its cooler surroundings, which will getting warmer by absorbing the emitted radiation. However, we don't see the surroundings of our heat source getting warmed up and only see a minor temperature difference in figure 4.4. This is caused by our non-isolated cooled walls in the model, where we lose a lot of the transported radiative heat in positive and negative direction.

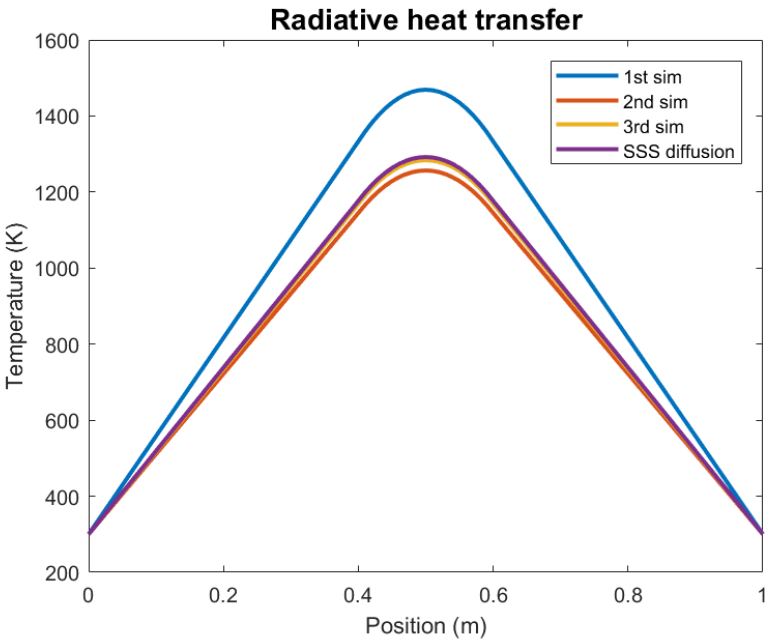

Figure 4.4: Radiative heat transfer model

4.3. Isolated wall

To prevent all the energy from escaping and to see how the intensities change for an isolated wall, we changed the right boundary condition to Neumann: no heat enters or leaves the furnace through the wall at $x = 1$. The results of this partially isolated furnace tends to approach the real industrial furnaces, since the companies are of course trying not to lose energy in the combustion process. This adaptation

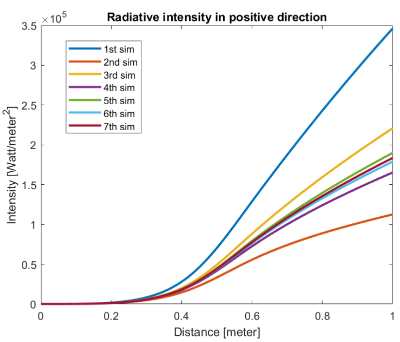

Figure 4.5: Radiative intensity in positive direction

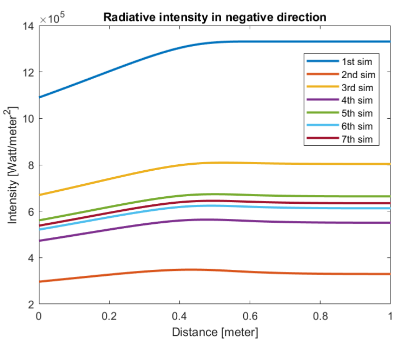

Figure 4.6: Radiative intensity in negative direction

also changes the behaviour of both radiative intensities, as can be seen in figure 4.5 and 4.6.

When looking at the radiative intensities, we observe that the intensity in positive direction keeps increasing towards the right boundary. The increase is caused by the high temperatures at the right half of the furnace. These high temperatures cause an extra high black body intensity, which dominates the slope of the radiative intensity.

In negative direction, because of the right boundary condition of the RTE (formula 2.13), the radiative flux leaving the rightside wall equals the black body intensity. Because of this, both terms in the RTE are (more or less) equal, which is why we see an (almost) horizontal intensity at the rightside of the furnace in figure 4.6.

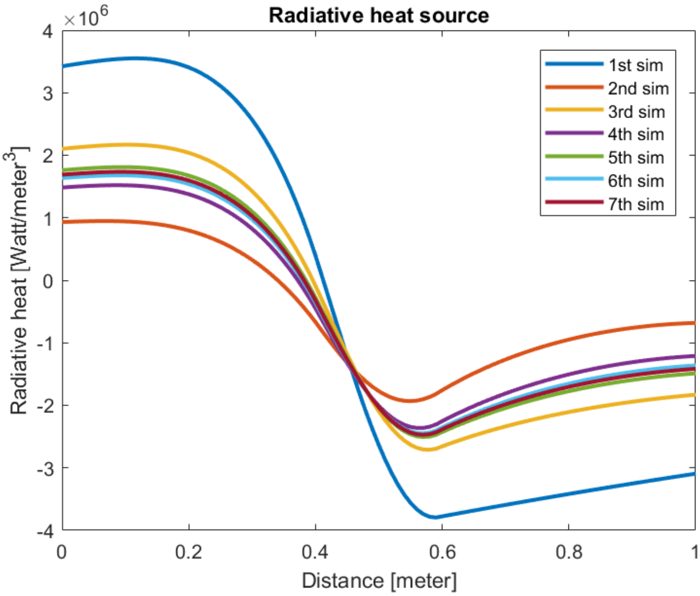

Figure 4.7: The contribution of the radiative heat transfer to the heat source

In figure 4.7 we can see the contribution of the radiative heat transfer to the heat source. In other words, this graph shows us the transport of thermal energy by radiation. Indeed, we can see the hot medium emitting a lot of electromagnetic radiation, which makes the medium cool down (negative heat). This heat is transported to the cooler surroundings at the leftside of the furnace, where the incident radiation is absorbed and converted it into heat. However, as can be seen in figure 4.6, because of the non-isolated wall at the leftside, this heat is transported outside of the furnace. The temperature distribution of the furnace with 1 isolated wall is shown in figure 4.8.

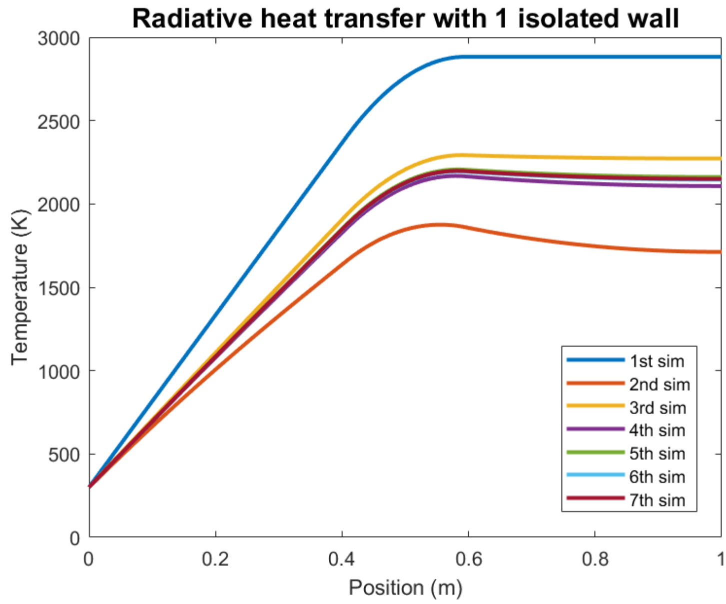

Figure 4.8: Radiative heat transfer model

The fluctuating of the solution until convergence is accomplished can be explained by mentioning that the flame in the middle of the furnace and radiation act as each others opposites. The first simulation is diffusion-only, which is why the temperature is too high. Because of this high temperature, there will be a lot of radiation pulling the temperature down in the second simulation. Because of the low temperature, radiation will do less in the third simulation, which is why the flame can heat the furnace again. This process continues till convergence is achieved.

4.4. Reflecting wall

Just as in subsection 3.2.3, the material of the walls can be of great influence on the radiative heat transfer in the furnace. We imitate the CONVERGE CFD model by setting the right wall emissivity $\epsilon = 0$. By the law of conservation of energy, the sum of the absorptivity, reflection and transmissivity is equal to 1 (figure 4.9). In this particular case, the quasi steady state situation, Kirchhoff's law of thermal radiation dictates that the absorptivity of the surface equals its emissivity. In other words, because of the non-transmissive assumption, setting $\epsilon = 0$ means that we have a 100% reflecting surface.

Since we have a wall on the rightside which is reflecting the electromagnetic waves, the intensity in negative direction now depends on the reflected incident radiation of the previous iteration. Running this simulation learns us that the reflection decreased the convergence speed of the discrete ordinates method. According to Balsara (2000) this is because the increased boundary condition impedes convergence: radiation in positive direction undergoes a reflection before leaving the domain. For this reason, the rate at which the right boundary converges diminishes and so does the convergence rate of the whole model.

In figure 4.10 we can see the effect of the wall emissivity: a temperature difference of almost 100 K at the center of the furnace. We can explain these results by looking at the intensity in negative direction. Because of the reflection, the radiative flux in this direction is considerably higher. We saw before that radiation transports heat from a hot body to its cooler surroundings. With a higher amount of radiation, naturally heat is transported faster from the warm areas to the cooler surroundings. On the other hand, despite the faster heat transfer, the core temperature of the furnace is considerably lower.

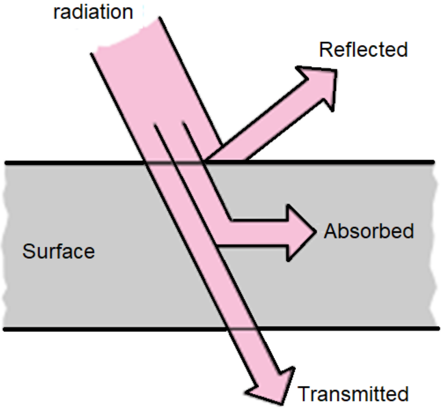

Figure 4.9: Radiation processes at a surface

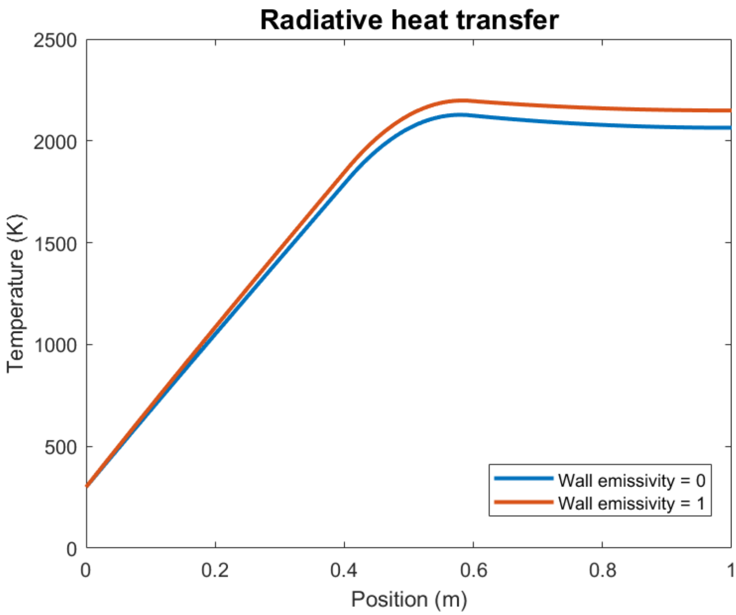

Figure 4.10: Radiative heat transfer model with different rightside wall emissivities

This gives immediately an interesting result for the large industrial furnaces. A wall emissivity of $\epsilon = 0$ transports the combustion heat faster through the whole furnace - this could be useful for indirect heating furnaces. However, a lot of companies use special high-emissivity coatings at the inside of the furnace, because a wall emissivity of $\epsilon = 1$ lets the furnace generate more heat without using more fuel. In these cases the fuel consumption can be reduced by using furnaces with a wall emissivity close to 1.

4.5. Weighted sum of grey gases

Finally, we included the weighted sum of grey gases model into our study (subsection 3.2.4). The WSGG replaces the nongrey gas in the radiative transfer equation by a number a grey gases, for which we calculate the intensities independently. This model is needed when the mixture of gases changes during a simulation. Because the MATLAB code is made for a quasi-steady state model, it does not make sense to let the gas mixture change over time in this implementation. However, we will use the WSGG to look into the influence of a different mixture of gases in the radiative heat transfer.

Just like in subsection 3.2.4, our first simulation will be with 22% O_2 and 78% N_2 in the air. Since the heaviside step function mimics the combustion of methane, we

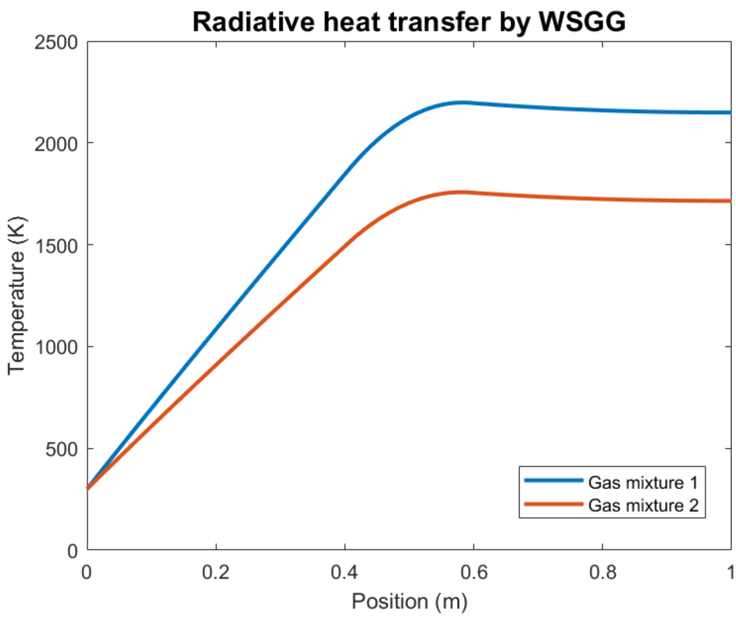

Figure 4.11: Radiative heat transfer model with different air mixtures

also consider the mixture of gases afterwards: 50% N_2, 27% CO_2 and 23% H_2O (based on the products of the chemical reaction).

Figure 4.11 shows us the visualisation of formula 2.12: the RTE's are linearly dependent on the absorption coefficient κ. The mean absorption coefficient in the second gas mixture is higher than in gas mixture 1, which results in radiation with higher intensities. As we learnt in the previous subsection, more radiation leads to more heat transfer from the warm bodies to outside the domain. This also confirms the observation in the CONVERGE CFD simulation that heat is transferred at a faster rate in the outlet gas stream, since the absorption coefficient is higher in that area. In general, we can conclude that, during the combustion process, the role of radiation in the transfer of heat is growing because of the changing mixture of gases in the furnace.

5 Conclusion

The main goal of this thesis was to model heat transfer by radiation in large industrial furnaces in an understandable way. In this conclusion we are making an overall conclusion by stating which tasks were accomplished and results have been shown in this report.

In the first part of this thesis, we pointed out the importance of the radiative heat transfer model and a thorough mathematical description of the theory on heat transfer has been made. The description considers the standard diffusive convective model as well as the transfer equations of the radiative model. To solve these equations, we chose the discrete ordinates method as a solving method. This method is based on discretization of the spatial dependence of the radiative intensity and evaluating a transport equation in every direction.

In the second part of this thesis, we used CONVERGE CFD and MATLAB software to numerically make several simulations of the combustion of methane in a one-dimensional quasi-steady state and in a three-dimensional furnace. In the furnace, radiation transports heat from places with high temperatures to their cooler surroundings, after which these surroundings get warmer by absorbing the radiation. The effect of radiation is best visible when we have isolated walls in the furnace, otherwise the transported heat will end up outside of the furnace. Also the material of the walls is important: a low emissivity, and therefore a high reflectivity, causes a higher radiation level, which speeds up the heat transfer in the furnace. On the other hand, in this case more fuel has to be used to establish the same core temperature than in a furnace with highly emissive walls. Finally, the weighted sum of grey gases allowed us to change the mixture of air in the furnace during the process, due to combustion. When the mass fraction of the products H_2O and CO_2 get higher, we see that the role of radiation in the transfer of heat in these areas is getting bigger.

Acknowledgements

I would like to thank my review committee for taking the time to assess my report. In particular, I am very grateful to my supervisor, dr. D.J.P. Lahaye, for providing me with great guidance and a lot of enthusiasm during the process. I am also thankful for the assistance of Veeraraghavan Viswanathan, senior research engineer in the Convergent Science team from Linz, who helped me becoming familiar with the new software. Finally, the Delft University of Technology deserves praise for supplying me with very high-quality education, especially for the way they were able to continue all courses during the pandemic.

Bibliography

[1] Balsara, Dinshaw (2000). *Fast and accurate discrete ordinates methods for multidimensional radiative tranfer. Part I, basis methods*. Journal of Quantitative Spectroscopy & Radiative Transfer, volume 69, pp. 671-707.

[2] Chmielewski, M. & Gieras, M. (2015). *Planck mean absorption coefficients of H_2O, CO_2, CO and NO for radiation numerical modeling in combustion flows.* Journal of Power Technologies, volume 95, pp. 97-104.

[3] Hurley, M.J. (2016). *SFPE Handbook of fire protection engineering*. Berlin: Springer.

[4] Knaus, H. et al. (1997). *Comparison of different radiative heat transfer models and their applicability to coal-fired utility boiler simulation*. 4th International Conference on Technologies and Combustion for a Clean Environment.

[5] Modest, M.F. (1991). *The weighted-sum-of-gray-gases model for arbitrary solution methods in radiative transfer*. Journal of Heat Transfer, volume 113, pp. 650-656.

[6] Modest, M.F. (2003). *Radiative heat transfer*. San Diego: Academic Press.

[7] Modest, M.F. & D.C. Haworth (2015). *Radiative heat transfer in turbulent combustion systems*. San Diego: Academic Press. New York: Springer.

[8] Nakate, P. & Lahaye, D. & Vuik, C. & Talice, M. (2021). *Analysis of the Aerodynamics in the Heating Section of an Anode Baking Furnace Using Non-Linear Finite Element Simulations*. Fluids 2021, volume 6.

[9] Selçuk, N. & Kayakol, N. (1997). *Evaluation of discrete ordinates method for radiative transfer in rectangular furnaces*. International Journal of Heat and Mass Transfer, volume 40, pp. 213-222.

[10] Solomenko, Z. (2019). *Heat transfer with radiation in participating media and the discrete ordinates method*. comsol.de, accessed July 25th 2021.

[11] Thynell, S.T. (1998). *Discrete-ordinates method in radiative heat transfer*. International Journal of Engineering Science, volume 36.

[12] Versteeg, H.K. & Malalasekera, W. (2007). *An introduction to computational fluid dynamics.* Harlow: Pearson Education Limited.

[13] Zhang, H. & Modest, M.F. (2001). *Evaluation of the Planck-mean absorption coefficients from HITRAN and HITEMP databases*. Journal of Quantitative Spectroscopy & Radiative Transfer, volume 73, pp. 649-653.